Sequential Construction Strategy for Rational Design of Luminescent Iridacycles

Hui Xu,[†,||] Zi-Ao Huang,[†,||] Xugeng Guo,[†,§] Yuhui Yang,[†] Yuhui Hua,[†,‡] Zexing Cao,[†,§] Shunhua Li,*[,†,‡] and Haiping Xia*[,†]

[†]State Key Laboratory for Physical Chemistry of Solid Surfaces, Collaborative Innovation Center of Chemistry for Energy Materials and College of Chemistry and Chemical Engineering, Xiamen University, Xiamen 361005, China

[‡]The MOE Key Laboratory of Spectrochemical Analysis & Instrumentation, Xiamen 361005, China

[§]Fujian Provincial Key Laboratory of Theoretical and Computational Chemistry, Xiamen University, Xiamen, 361005, China

S *Supporting Information*

ABSTRACT: A convenient and general strategy has been developed to synthesize stable iridapolycycles **5−8**. Reaction of arylacetylenes with iridium-hydride complex [IrH(CO)Cl(PPh$_3$)$_3$]-BF$_4$ via nucleophilic addition, oxidative decarbonylation, and C−H bond activation results in the formation of a series of iridacyclopentadiene derivatives, including benzo-iridacyclopentadiene **5**, naphtho-iridacyclopentadiene **6**, pyreno-iridacyclopentadiene **7**, and thieno-iridacyclopentadiene **8**. These iridapolycycles display high thermal and air stability yet can be further functionalized via facile ligand substitution reactions. As an example, complex **5** was used as a metallosynthon to react with 2,2′-dipyridyl to give intensely luminescent Ir(III) complex **9** bearing one C^C and one N^N ligands. Density functional theory (DFT) calculations reveal that the lowest unoccupied molecular orbitals (LUMOs) of iridapolycycles **5−8** are located on the phosphonium groups while the highest occupied molecular orbitals (HOMOs) are mainly located on the metal-embedded C^C frameworks. Our method offers a sequential construction strategy for constructing luminescent iridacycles, which potentially allows facile tuning of the photoluminescence properties by modulating the C^C and N^N moieties independently.

INTRODUCTION

In the recent two decades, iridium(III) complexes have been attracting increasing research interest because of their significant luminescent features, such as efficient triplet-state phosphorescence[1] and tunable emission covering the visible to near-infrared (NIR) region.[2] For example, Ir(III) complexes have been widely investigated as emissive dopants in organic light emitting devices (OLED),[3] nonlinear optical (NLO) materials,[4] photosensitizers,[5] luminescent chemosensors,[6] and biological labeling reagents.[7] Compared with organic fluorophores, cyclometalated Ir(III) complexes display relative long-lived emissions with usually larger Stokes shifts, which contribute to higher sensitivity and lower background in their photoluminescence responses.[2d] The photophysical properties of cyclometalated Ir(III) complexes are principally determined by the cyclometalating ligand.[1b,e] In pursuit of a highly emissive Ir(III) complex, great efforts have been devoted to Ir(III) complexes that bear phenylpyridine-based cyclometalating ligand.[1d,g] In a sharp contrast, luminescent Ir(III) complexes with a C^C framework are greatly under-explored, in spite of the rapid development of iridacycles chemistry over the past several decades.[8] Although many iridacycles such as five-membered iridacyclopentadiene and its derivatives have been synthesized and characterized, their photophysical properties
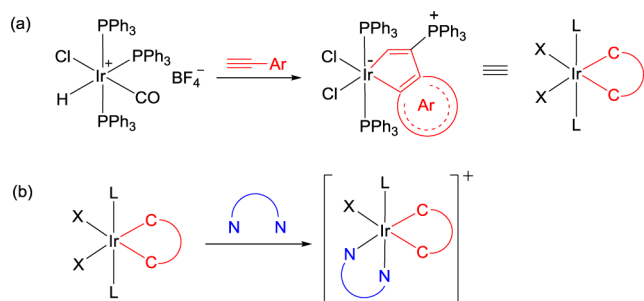
have rarely been reported. Herein, we report a general and robust strategy to synthesize a series of stable polycyclic Ir(III) complexes bearing bidentate cyclometalated C^C frameworks. Further functionalization of these iridacycles via facile ligand substitution reactions results in highly luminescent Ir(III) complexes.

In our previous study, we found that introduction of a phosphonium group onto the C^C framework greatly contributes to the stabilization of metallacycles.[9] This strategy is now utilized to synthesize iridapolycycles. Reaction of iridium-hydride complex [IrH(CO)Cl(PPh$_3$)$_3$]BF$_4$ with arylacetylenes via nucleophilic addition, oxidative decarbonylation, selective C−H bond activation, and dehydrogenation results in the highly stable iridapolycycles (i.e., (C^C)IrCl$_2$(PPh$_3$)$_2$) (Scheme 1a). Further treatment of the iridapolycycle **5** with 2,2-bipyridyl led to the replacement of one chloride and one PPh$_3$ ligand to give the heteroleptic Ir(III) complex (i.e., [(C^C)(N^N)IrClPPh$_3$]$^+$) (Scheme 1b). The substitution product **9** exhibits efficient photoluminescence with large Stokes shift and relatively long lifetime compared with organic

Scheme 1. Schematic Illustration of the Sequential Synthesis of (a) (C^C)IrCl$_2$(PPh$_3$)$_2$ and (b) [(C^C)(N^N)IrClPPh$_3$]$^+$

Figure 1. Molecular structure of complex **1** (50% probability thermal ellipsoids). The counteranion and phenyl moieties in PPh3 are omitted for clarity. Selected bond distances [Å] and angles [deg]: Ir1−C1 = 2.127(4), C1−C2 = 1.332(5), C2−C3 = 1.503(5), Ir1−C9 = 1.837(4), Ir1−P1 = 2.3678(10), Ir1−P2 = 2.3567(10), Ir1−Cl1 = 2.4033(9), C2−C1−Ir1 = 136.1(3), C1−C2−C3 = 127.2(3), and P1−Ir1−P2 = 166.15(3).

fluorophores, which are characteristics of the phosphorescence of cyclometalated Ir(III) complexes.[10]

Compared with the traditional way to synthesize C^N based phosphorescent Ir(III) complexes via the Nonoyama route,[11] our strategy is to construct C^C and N^N frameworks sequentially, allowing more flexibility in both synthesis and modification.

■ RESULTS AND DISCUSSION

In general, the preparation of heteroleptic (C^C)IrCl$_2$(PPh$_3$)$_2$ involves a two-step procedure. First, [IrH(CO)Cl(PPh$_3$)$_3$]BF$_4$ was treated with arylacetylenes such as phenylacetylene, 2-ethynylnaphthalene, 1-ethynylpyrene, and 2-ethynylthiophene in CHCl$_3$ at room temperature for 2 h to give complexes **1**, **2**, **3**, and **4**, respectively, in high yields (Scheme 2).
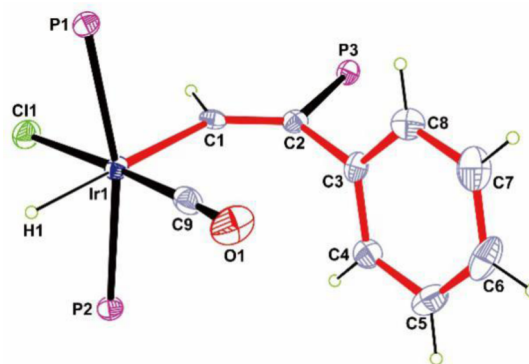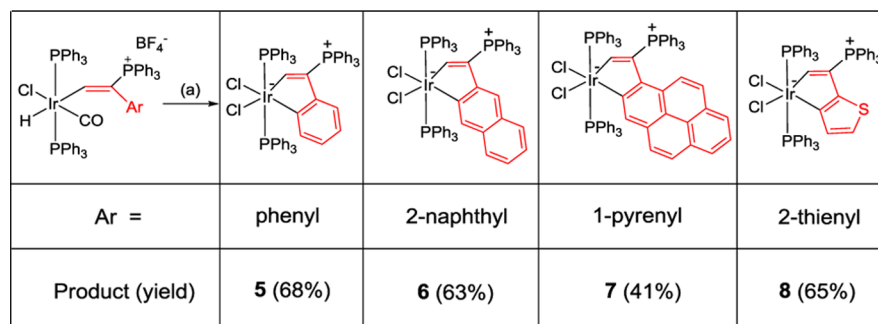
Scheme 2. Preparation of Iridium Vinyl Complexes 1, 2, 3, and 4

Ar =	phenyl	2-naphthyl	1-pyrenyl	2-thienyl
Product (yield)	**1** (95%)	**2** (92%)	**3** (90%)	**4** (93%)
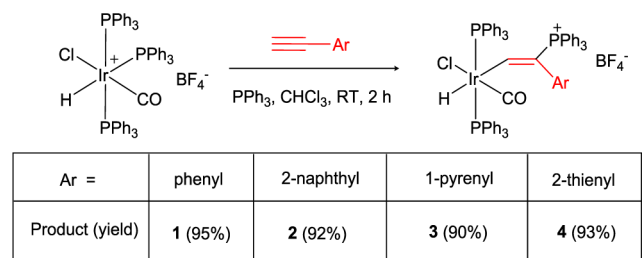
An X-ray single-crystal diffraction experiment has been carried out to clarify the structure of **1**. As shown in Figure 1, the geometry of the iridium center can be viewed as an octahedron in which the six coordination sites are occupied by C1, one hydrogen atom, one chloride atom, the carbon atom of the carbonyl ligand, and two phosphorus atoms of the phosphine ligands. The Ir1−C1 (2.127(4) Å) bond is of a typical length for Ir−C single bond, and the C1−C2 (1.332(5) Å) bond is of a typical length for the C=C double bond.[12]

The solution NMR spectroscopic data of **1** are consistent with its solid-state structure. In particular, the ^{1}H NMR spectrum of **1** shows the characteristic IrCH signal at δ = 10.1 ppm and the IrH signal at δ = −8.3 ppm. In the ^{31}P NMR spectrum, the signals for CPPh_3 and IrPPh_3 are observed at δ = 19.7 ppm and δ = −0.93 ppm, respectively. In the ^{13}C NMR spectrum, the characteristic carbon signals are observed at δ = 186.7 (IrCH), 163.3 (CO), and 122.2 (CPPh_3) ppm, respectively.

The ^{1}H NMR spectral behaviors of **2**, **3**, and **4** are very similar to that of **1**. The characteristic proton signals for IrCH
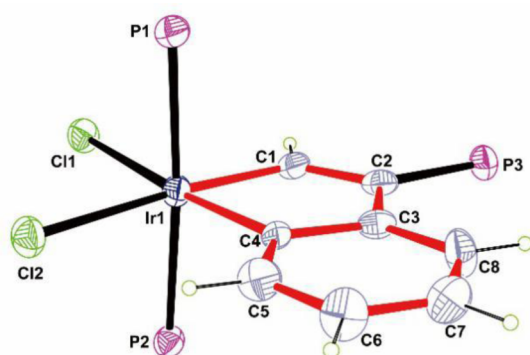
and IrH are observed at δ = 10.2 (**2**), 10.7 (**3**), 10.2 ppm (**4**), and δ = −8.3 (**2**), − 8.7 (**3**), and − 8.1 ppm (**4**), respectively. The ^{31}P NMR spectra of **2** and **4** show the CPPh_3 signals at δ = 19.6 and 19.5 ppm and the IrPPh_3 signals at δ = −0.78 and − 0.59 ppm, respectively. However, the ^{31}P NMR spectral behavior of **3** is greatly different from those of **1**, **2**, and **4**. Two sets of IrPPh_3 signals appear at δ = 0.28 ppm and δ = −2.7 ppm with a large P−P coupling constant of 363.4 Hz. This is attributed to the bulky pyrenyl group in **3** which makes the two phosphine ligands asymmetrical (P1−Ir1−P2 = 160.97(4)°). The structure of **3** has also been determined by an X-ray diffraction study, and a view of the cation of **3** is shown in Figure S1.

Second, treatment of the chloroform solution of iridium vinyl complexes **1**, **2**, **3**, or **4** with trimethylamine-N-oxide (TMAO) and tetrabutylammonium chloride at 80 °C resulted in the expected loss of the CO ligand[13] and the following C−H activation,[14] leading to the formation of highly stable iridapolycycles **5**, **6**, **7**, or **8** (Scheme 3), respectively. The decarbonylation of metal carbonyls via CO$_2$-generated oxidative elimination is a useful synthetic strategy that can be effected with oxygen-atom donors such as amine oxides.[13b] In our synthetic route, TMAO is used as the decarbonylation reagent, and the dehydrogenation preference should be the driving force for the selective *ortho* C−H activation.

The structure of **5** has been determined by an X-ray diffraction study. As shown in Figure 2, the geometry of the iridium center can be viewed as an octahedron in which the six coordination sites are occupied by C1, C4, two chloride atoms, and two phosphorus atoms of the triphenylphosphine ligands. Complex **5** contains a basic planar iridabicyclic ring, and the mean deviation from the least-squares plane through Ir1 and C1−C8 is 0.0088 Å. The sum of the angles in the five-membered iridacycle is 539.9°, which is very close to the ideal value of 540°. In the five-membered iridacycle, the two Ir−C bond lengths are 1.977(8) (Ir1−C1) and 2.033(7) (Ir1−C4) Å. The other three C−C distances within this ring are 1.378(10) (C1−C2), 1.500(9) (C2−C3), and 1.427(9) Å) (C3−C4). The two triphenylphosphine ligands are mutually *trans* with Ir−P distances of 2.3461(18) and 2.3435(17) Å. The two Ir−Cl distances are 2.5053(16) and 2.4967(18) Å.

Scheme 3. Synthesis of Iridapolycycles 5, 6, 7, and 8[a]

Ar =	phenyl	2-naphthyl	1-pyrenyl	2-thienyl
Product (yield)	**5** (68%)	**6** (63%)	**7** (41%)	**8** (65%)

[a]Note: (a) $(CH_3)_3NO$, Bu_4NCl, $CHCl_3$, 80 °C, 24 h.

Figure 2. Molecular structure of complex **5** (50% probability thermal ellipsoids). Phenyl moieties in PPh_3 are omitted for clarity. Selected bond distances [Å] and angles [deg]: Ir1−C1 = 1.977(8), Ir1−C4 = 2.033(7), C1−C2 = 1.378(10), C2−C3 = 1.500(9), C3−C4 = 1.427(9), C4−C5 = 1.392(9), C5−C6 = 1.386(10), C6−C7 = 1.392(11), C7−C8 = 1.402(11), C8−C3 = 1.389(10), Ir1−P1 = 2.3461(18), Ir1−P2 = 2.3435(17), Ir1−Cl1 = 2.5053(16), Ir1−Cl2 = 2.4967(18), C1−Ir1−C4 = 79.9(3), C2−C1−Ir1 = 119.2(5), C1−C2−C3 = 112.9(6), C2−C3−C4 = 112.1(6), C3−C4−Ir1 = 115.8(5), and P1−Ir1−P2 = 175.61(6).

Consistent with its solid-state structure, the ^1H NMR spectrum of **5** shows the characteristic IrCH signal at δ = 10.1 ppm. The signals for the remaining four protons of the six-membered ring resonate appear at 6.3, 6.2, 6.0, and 5.7 ppm, which shift to high field compared with the signals of benzene.

In the ^{31}P NMR spectrum, the signals for CPPh_3 and IrPPh_3 are observed at δ = 10.2 ppm and δ = −5.8 ppm, respectively. In the ^{13}C NMR spectrum, the characteristic carbon signals for the five-membered iridacycle are observed at δ = 197.1 (IrCH), 151.6 (IrCHC(PPh$_3$)C), 146.1 (IrC), and 115.8 (IrCHC(PPh$_3$)) ppm. The remaining four carbon signals for the six-membered ring appear at 134.8, 124.4, 120.4, and 119.4 ppm.

The benzo-iridacyclopentadiene **5** has a framework of two fused rings, which can be viewed as iridaindene. Some of iridaindene complexes had been reported before. Ir[C$_8$H$_5$(Ph-2)](C$_5$H$_5$)(P^{i}Pr$_3$) was prepared from vinyl complex Ir(PhC= CHPh) (OCOCF$_3$)(C$_5$H$_5$)(P^{i}Pr$_3$) reacted with NH$_4$PF$_6$ in methanol.[15] Wright and co-workers reported the synthesis of 1-iridaindene Ir[C$_8$H$_5$(Ph-3)]Cl(PPh$_3$)$_2$ from IrHCl$_2$(PPh$_3$)$_3$ and organomercury compound Hg(CH=CPh$_2$)$_2$.[16] Choudhury reported the synthesis of another 1-iridaindene Ir[C$_8$H$_5$(Ph-2)]Cl(PPh$_3$)$_2$ from the reaction of IrCl(PPh$_3$)$_3$ with diphenyldiacetylene.[17] Recently, Paneque reported the synthesis of β-metallanaphthalene by insertion of the olefin into the iridaindene Tp^{Me2}Ir[C$_6$H$_4$-o-C(CO$_2$Me) C(CO$_2$Me)]-(OH$_2$).[18]

A plausible mechanism for the formation of iridaindene **5** is proposed in Scheme 4. The iridium-hydride complex [IrH-(CO)Cl(PPh$_3$)$_3$]BF$_4$ undergoes coordination of the ethynyl and dissociation of a PPh$_3$ ligand to give **A**. Subsequently, the nucleophilic attack of the free PPh$_3$ on the β-carbon of the ethynyl results in iridium vinyl complex **1**. The oxidative decarbonylation of **1** by TMAO leads to the 16e-unsaturated

**Scheme 4. Plausible Mechanism for the Formation of Complex 5**
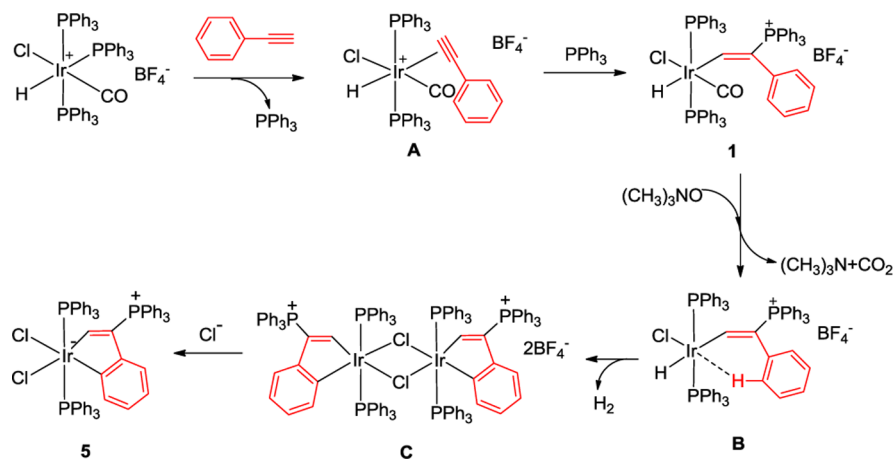
agostic intermediate **B**. Activation of the *ortho* C−H bond in **B** by the iridium center and the following dehydrogenation step led to the dichlorido-bridged dimer **C**.[14a] We carried out the measurement of the gaseous products by gas chromatography. The GC chromatograms are depicted in Figure S9. The result clearly confirms the production of H_2 gas during the reaction. Finally, coordination of chloride anions onto the 16e-unsaturated Ir centers of the dimer gives the observed product **5**.

Similarly, naphtho-iridacyclopentadiene **6**, pyreno-iridacyclopentadiene **7**, and thieno-iridacyclopentadiene **8** were synthesized by varying the arylacetylenes. The structures of **6**, **7**, and **8** have also been determined by an X-ray diffraction study (Figure S2−S4) and NMR characterization (see Experimental Section). Unfortunately, the poor solubility of **7** prevented the ^{13}C NMR characterization.

The thermal stability of the iridapolycycles **5**−**8** was evaluated by NMR studies. The thermal stability tests of **5**−**8** in solid state have been performed in air, and the results are summarized in Table S2. These new species of iridapolycycles containing an iridacyclopentadiene moiety display remarkable stability. The solid sample of **5** or **6** can be heated at 200 °C for at least 8 h without noticeable decomposition, and the solid sample of **7** or **8** remains unchanged under heating at 150 °C for at least 8 h. When the temperature was increased to 170 °C, the sample of **7** or **8** partly decomposed. The thermal stability tests of **5**−**8** in solution have also been studied. Comparison of the thermal stability of these iridapolycycles in DMF is presented in Table S3. It is noteworthy that heating the solution of **5** or **6** at 120 °C did not result in noticeable decomposition.

Finally, ligand substitution reactivity of the synthesized iridapolycycles were further invesitgated. Treatment of **5** with 2,2′-dipyridyl led to the replacement of one chloride and one PPh₃ ligand to give complex **9** (Scheme 5). The structure of **9**

**Scheme 5. Preparation of Ir(III) Complex 9**
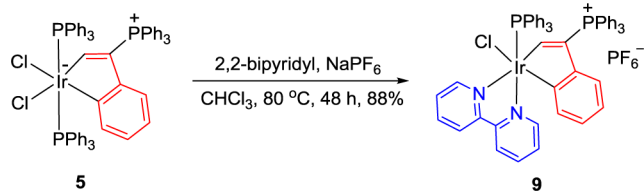
has been determined by NMR spectra and an X-ray diffraction study. As shown in Figure 3, the geometry of the iridium center of **9** can also be viewed as an octahedron, which is similar to that of **5**. The structural parameters of the iridaindene framework keep almost unchanged after the ligand substitution reaction. It should be noted that the Ir1−N2 length (2.088(7) Å) is shorter than the length of Ir1−N1 (2.157(7) Å) because of the different steric influences of the PPh₃ ligand and the C^C framework.

The absorption spectra of iridapolycycles **5**−**8** are depicted in Figure 4a. With the extension of the iridium-embedded fused rings, both the red shift of the lowest-energy absorption bands and the increase of the molar extinction coefficient are observed. For example, **7** displays broader and stronger absorption due to its extended π-conjugated system, and the metal-to-ligand charge-transfer (MLCT) absorption peak appears at 443 nm. The absorption behavior of **5** is very similar to that of **8**, which is also dominated by an iridabicyclic
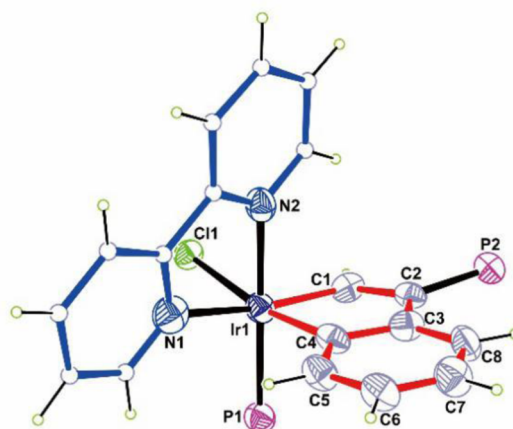
Figure 3. Molecular structure of complex **9** (50% probability thermal ellipsoids). The counteranion and phenyl moieties in PPh₃ are omitted for clarity. Selected bond distances [Å] and angles [deg]: Ir1−C1 = 1.981(7), Ir1−C4 = 2.027(7), C1−C2 = 1.378(10), C2−C3 = 1.462(10), C3−C4 = 1.422(10), Ir1−P1 = 2.284(2), Ir1−Cl1 = 2.5057(16), Ir1−N1 = 2.157(7), Ir1−N2 = 2.088(7), C1−Ir1−C4 = 80.7(3), C2−C1−Ir1 = 116.2(5), C1−C2−C3 = 115.7(6), C2−C3−C4 = 112.1(6), C3−C4−Ir1 = 115.0(5).
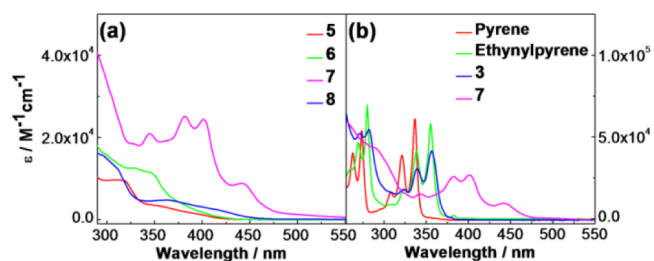
Figure 4. (a) Absorption spectra of complexes **5**−**8** recorded in CH_2Cl_2 solution at room temperature. (b) Absorption spectra of pyrene, ethynylpyrene, **3**, and **7** recorded in CH_2Cl_2 solution at room temperature.

chromophore. A comparison of the absorption of pyrene, ethynylpyrene, **3**, and **7** is shown in Figure 4b. A strong multiple absorption band with the fine vibration structure, which results from the π → π* transition of the rigid, planar, and conjugated pyrene-derived chromophores, appears in all of these four complexes. The π → π* absorption band of ethynylpyrene or **3** displays a red shift compared with that of pyrene as the ethynyl or vinyl group extends the π conjugation. After the C−H activation and the resulting formation of complex **7**, the characteristic absorption band shows a further red shift, the vibration structure is slightly blunted, and an additional MLCT absorption band appears as the lowest-energy band, as reflected by its remarkable solvent-dependent shift (Figure S5). The simulated absorption spectra of complexes **5**−**9** by time-dependence density functional theory (TD-DFT) calculations with the B3LYP functional are shown in Figure S10. The computational results match the experimental absorption behaviors very well.

The photoluminescence spectra of **5**, **6**, **7**, and **8** are recorded in CH_2Cl_2 at room temperature (Figure 5). Obvious red shifts are observed with the increase of an extended π-conjugated system of the C^C framework. Compared with **5**, another iridabicycle **8** diplays stronger photoluminescence with a remarkable red shift and a larger Stokes shift. Green and red
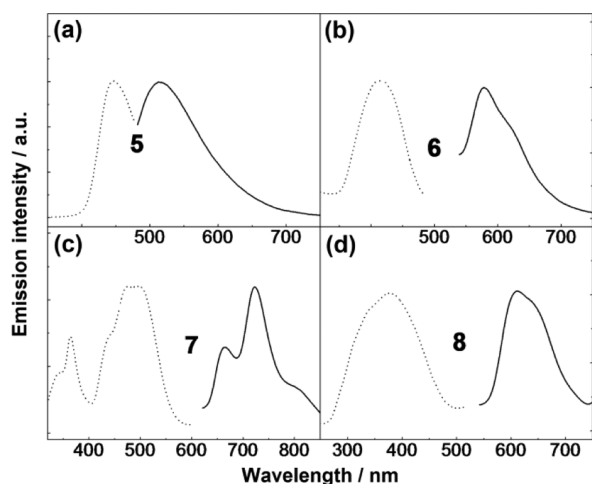
Figure 5. Excitation (dot) and emission (solid) spectra of (a) **5**, (b) **6**, (c) **7**, and (d) **8** recorded in CH_2Cl_2 solution at room temperature.

emissions are observed from the solids of **5** and **8**, respectively, upon irradiation at 365 nm (Figure S6), which is consistent with the solution spectra depicted in Figure 5.

To better understand the photophysical properties of the synthesized iridapolycycles, the energy levels and electron density distributions of their molecular orbitals were estimated. By referring to the X-ray diffraction data, we performed the density functional theory (DFT) calculations at the B3LYP/[LANL2DZ+6-31G*] level of theory. The optimized geometries and extended frontier orbitals of the investigated iridapolycycles **5−9** are given in Figure 6, and the calculated HOMO and LUMO levels of **5−9** are summarized in Table 1.

The calculation results show that the lowest unoccupied molecular orbitals (LUMOs) of complexes **5−8** are located on the phosphonium groups while the highest occupied molecular orbitals (HOMOs) mainly concentrate on the planar metal-embedded C^C frameworks. For complex **8**, the introduction of the electron-donating sulfur atom into the C^C framework raises its HOMO level, inducing a smaller energy gap than that of complex **5**. These results demonstrate that the C^C ligands play an important role in the modulation of the emission color, showing good agreement with the experimental observations described above.[19]

Compared with **5**, its ligand substitution product **9** displays a red-shifted emission (λ_{em} = 570 nm) in air with a remarkable enhancement in intensity (Figure 7a). The quantum yield (QY) of **5** in deaerated CH_2Cl_2 solution is lower than 0.01, while **9** diplays a high QY of 0.72 in deaerated CH_2Cl_2 solution at room temperature. As shown in Figure S7, intense yellow emission can be observed from the solid state and solution of **9** upon ultraviolet excitation. DFT calculations reveal that the LUMO of **9** is located on the N^N ligand, while the HOMO still mainly concentrates on the metal-embedded C^C framework (Figure 6). The luminescence enhancement observed from **9** is therefore explained in terms of the LUMO shift from the phosphonium group to the rigid N^N ligand. The HOMO and LUMO are located on the C^C and N^N moieties, respectively, indicating the possibility of facile modulation of the luminescence properties of this type of heteroleptic Ir(III) complexes.

Emission decay curves of **9** in deaerated and air-saturated CH_2Cl_2 at room temperature are depicted in Figure S8. The photoluminescence lifetime of **9** is at the level of 10^{-7} s, which
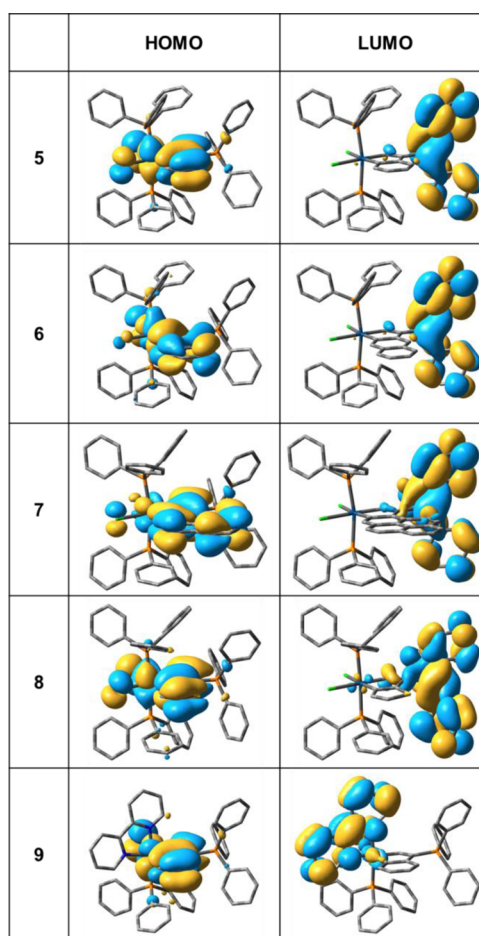
Figure 6. Calculated HOMO/LUMO distributions of complexes **5−9**.

Table 1. Calculated HOMO and LUMO Levels of the Complexes 5−9

	LUMO (eV)	HOMO (eV)	energy gap (eV)
5	−1.511	−4.679	3.168
6	−1.547	−4.706	3.159
7	−1.562	−4.562	3.001
8	−1.510	−4.540	3.031
9	−4.419	−7.310	2.891
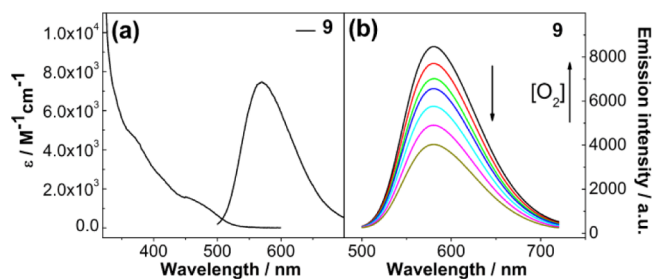
Figure 7. (a) Absorption and emission spectra of complex **9** recorded in CH_2Cl_2 solution at room temperature. (b) Emission spectral traces of complex **9** in deaerated CH_2Cl_2 solution (3.0×10^{-4} mol/L) upon increasing exposure to air. The emission spectra were recorded at 365 nm excitation.

is typical of the phosphorescence of cyclometalated Ir(III) complex. In accord with the relatively long emission lifetime, a significant dynamic quenching effect of oxygen is observed.

Upon exposure to air, the deaerated solution of **9** displays an obvious decrease of the luminescence (Figure 7b) accompanied by a reduction of the emission lifetime from 438 to 257 ns (Figure S8). The QY of **9** in air-saturated CH_2Cl_2 is measured to be 0.10, which is much lower than that in deaerated CH_2Cl_2. This indicates that the synthesized Ir(III) complex **9** could potentially serve as a sensitive luminescent sensor for use in naked-eye detection of O_2.

CONCLUSIONS

In summary, we have developed a general and robust strategy to the synthesis of four iridapolycycles **5−8**. These iridapolycycles bearing different π-conjugated C^C fragments show high thermal stability in air. As the bipyridyl-derived product of **5**, the heteroleptic Ir(III) complex **9** exhibits intense yellow photoluminescence with large Stokes shift and relatively long lifetime which are typical of the phosphorescence from cyclometalated Ir(III) complexes. DFT calculations reveal that the LUMO of complex **5** is located on the N^N ligand, and the HOMO is mainly located on the metal-embedded C^C frameworks, while the LUMO of complex **9** resides on the N^N ligand. Our method offers a sequential construction strategy for constructing luminescent iridacycles, which potentially allows facile tuning of the photoluminescence properties by modulating the C^C and N^N moieties independently. Furthermore, the subsidiary ligands (chloride and PPh_3) of this type of Ir(III) luminophores possess additional ligand substitution reactivities and thus offer a second functionalization site, which is abundant in stereochemical activity, for potential sensing or imaging applications in chemical biology.

EXPERIMENTAL SECTION

Syntheses and Materials. All manipulations were carried out under an inert atmosphere (Ar or N_2) by means of standard Schlenk techniques. Solvents were distilled from sodium/benzophenone (hexane and diethyl ether) or calcium hydride (dichloromethane and chloroform) under N_2 prior to use. The starting materials $[IrH(CO)Cl(PPh_3)_3]BF_4$, 2-ethynylnaphthalene, 1-ethynylpyrene, and 2-ethynylthiophene were synthesized by the previously published procedures.[20]

Characterizations. NMR spectroscopic experiments were carried out on Bruker Avance II 400 MHz, Bruker Avance III 500 MHz, and Bruker Avance III 850 MHz spectrometer. ^{1}H and ^{13}C NMR chemical shifts are relative to TMS, and ^{31}P NMR chemical shifts are relative to 85% H_3PO_4. High resolution mass spectra (HR-MS) were recorded on a Bruker En Apex ultra 7.0T FT-MS mass spectrometer. Absorption and fluorescence spectra were recorded on a Hitachi U-3900 ultraviolet−visible spectrophotometer and a Hitachi F-7400 fluorophotometer, respectively. The emission decay times were acquired with a HORIBA Jobin Yvon FluoroMax-4 TCSPC time-resolved fluorophotometer, which was equipped with an F-3018 integrating sphere accessory and further employed to measure the absolute fluorescence quantum yields by the integrating sphere approach.

Theoretical Calculations. The DFT calculations have been performed for geometry optimizations of complexes **5−9** using the B3LYP functional[21] with the basis set of LANL2DZ for Ir, P, and Cl atoms and the 6-31G* basis set for other atoms implemented in the Gaussian 09 package.[22] Polarization functions of Ir (ζ(d) = 0.938), P (ζ(d) = 0.340), and Cl (ζ(d) = 0.514) are also incorporated into the LANL2DZ basis set.[23] In addition, the TD-DFT calculations have been used to simulate their absorption spectra at the same density functional and basis set.

Preparation of Iridium Vinyl Complex 1. Phenylacetylene (53 μL, 0.48 mmol) and PPh_3 (346 mg, 1.32 mmol) were added to a solution of $[IrH(CO)Cl(PPh_3)_3]BF_4$ (500 mg, 0.44 mmol) in chloroform (10 mL). The mixture was stirred at room temperature (RT) for 2 h to
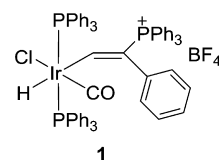

1

give a colorless solution. The solvent was removed under vacuum. The residue was washed with diethyl ether (3 × 10 mL) and dried under vacuum to give **1** as a white solid (520 mg, 95%). ^{1}H NMR (500.2 MHz, $CDCl_3$): δ = 10.1 (d, $^3J_{PH}$ = 36.9 Hz, 1 H, IrC**H**), 6.1−7.8 (m, 50 H, PPh_3 and Ph), −8.3 ppm (td, $^2J_{PH}$ = 15.8 Hz, $^4J_{PH}$ = 15.5 Hz, 1 H, Ir**H**). ^{31}P NMR (202.5 MHz, $CDCl_3$): δ = 19.7 (s, CPPh_3), −0.93 ppm (s, IrPPh_3). ^{13}C NMR plus HSQC (125.8 MHz, $CDCl_3$): δ = 186.7 (m, IrCH), 163.3 (t, $^2J_{PC}$ = 7.2 Hz, CO), 118.0−138.0 (m, PPh_3 and Phenyl), 122.2 ppm (d, $^1J_{PC}$ = 56.3 Hz, IrCHC(PPh_3)). HR-MS (ESI): m/z [M]$^+$ calcd for $C_{63}H_{52}ClIrOP_3$ 1145.2544, found 1145.2541. Anal. Calcd for $C_{63}H_{52}BClF_4IrOP_3$: C, 61.39; H, 4.25. Found: C, 61.50; H, 4.36.


2
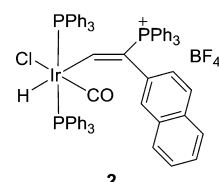
Preparation of Iridium Vinyl Complex 2. 2-Ethynylnaphthalene (68 μL, 0.48 mmol) and PPh_3 (346 mg, 1.32 mmol) were added to a solution of $[IrH(CO)Cl(PPh_3)_3]BF_4$ (500 mg, 0.44 mmol) in chloroform (10 mL). The workup method for **1** was used to give **2** as a light yellow solid (522 mg, 92%). ^{1}H NMR (850.3 MHz, CD_2Cl_2): δ = 10.2 (d, $^3J_{PH}$ = 36.8 Hz, 1 H, IrC**H**), 6.1−7.9 (m, 52 H, PPh_3 and naphthyl), −8.3 ppm (td, $^2J_{PH}$ = 15.4 Hz, $^4J_{PH}$ = 15.6 Hz, 1 H, Ir**H**). ^{31}P NMR (202.5 MHz, CD_2Cl_2): δ = 19.6 (s, CPPh_3), − 0.78 ppm (s, IrPPh_3). ^{13}C NMR plus HSQC (213.8 MHz, CD_2Cl_2): δ = 186.5 (m, IrCH), 163.6 (t, $^2J_{PC}$ = 7.3 Hz, CO), 118.0−138.0 (m, PPh_3 and Naphthyl), 122.6 ppm (d, $^1J_{PC}$ = 55.8 Hz, IrCHC(PPh_3)). HR-MS (ESI): m/z [M]$^+$ calcd for $C_{67}H_{54}ClIrOP_3$ 1195.2700, found 1195.2696. Anal. Calcd for $C_{67}H_{54}BClF_4IrOP_3$: C, 62.74; H, 4.24. Found: C, 62.83; H, 4.04.
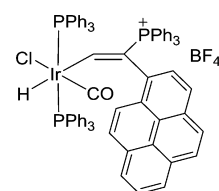

3

Preparation of Iridium Vinyl Complex 3. 1-Ethynylpyrene (108 mg, 0.48 mmol) and PPh_3 (346 mg, 1.32 mmol) were added to a solution of $[IrH(CO)Cl(PPh_3)_3]BF_4$ (500 mg, 0.44 mmol) in chloroform (10 mL). The workup method to **1** was used to give **3** as a light yellow solid (538 mg, 90%). ^{1}H NMR (500.2 MHz, CD_2Cl_2): δ = 10.7 (d, $^3J_{PH}$ = 37.6 Hz, 1 H, IrC**H**), 6.7−8.3 (m, 54 H, PPh_3 and pyrenyl), −8.7 ppm (td, $^2J_{PH}$ = 16.0 Hz, $^4J_{PH}$ = 16.7 Hz, 1 H, Ir**H**). ^{31}P NMR (202.5 MHz, CD_2Cl_2): δ = 19.5 (s, CPPh_3), 0.28(d, $^2J_{PP}$ = 363.4 Hz, IrPPh_3), −2.7 ppm (d, $^2J_{PP}$ = 363.4 Hz, IrPPh_3). ^{13}C NMR plus HSQC (213.8 MHz, CD_2Cl_2): δ = 189.5 (m, IrCH), 162.3 (t, $^2J_{PC}$ = 6.9 Hz, CO), 118.0−138.0 (m, PPh_3 and Pyr), 122.6 ppm (d, $^1J_{PC}$ = 54.0 Hz, IrCHC(PPh_3)). HR-MS (ESI): m/z [M]$^+$ calcd for $C_{73}H_{56}ClIrOP_3$ 1269.2857, found 1269.2852. Anal. Calcd for $C_{73}H_{56}BClF_4IrOP_3$: C, 64.63; H, 4.16. Found: C, 64.90; H, 4.16.

Preparation of Iridium Vinyl Complex 4. 2-Ethynylthiophene (48 μL, 0.48 mmol) and PPh_3 (346 mg, 1.32 mmol) were added to a solution of $[IrH(CO)Cl(PPh_3)_3]BF_4$ (500 mg, 0.44 mmol) in chloroform (10 mL). The workup method to **1** was used to give **4** as a white solid (507 mg, 93%). ^{1}H NMR (500.2 MHz, $CDCl_3$): δ =

4
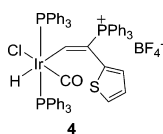
10.2 (d, $^3J_{PH}$ = 35.1 Hz, 1 H, IrCH), 5.9−7.9 (m, 48 H, PPh$_3$ and thienyl), −8.1 ppm (td, $^2J_{PH}$ = 15.1 Hz, $^4J_{PH}$ = 15.3 Hz, 1 H, IrH). ^{31}P NMR (202.5 MHz, CDCl$_3$): δ = 19.5 (s, CPPh$_3$), −0.59 ppm (s, IrPPh$_3$). ^{13}C NMR plus HSQC (125.8 MHz, CDCl$_3$): δ = 195.6 (br, IrCH), 162.8 (t, $^2J_{PC}$ = 7.1 Hz, CO), 118.0−140.0 (m, PPh$_3$ and thienyl), 114.9 ppm (d, $^1J_{PC}$ = 63.4 Hz, IrCHC(PPh$_3$)). HR-MS (ESI): m/z [M]$^+$ calcd for C$_{61}$H$_{50}$ClIrOP$_3$S 1151.2108, found 1151.2115. Anal. Calcd for C$_{61}$H$_{50}$BClF$_4$IrOP$_3$S: C, 59.16; H, 4.07. Found: C, 59.29; H, 4.08.
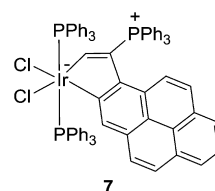

5
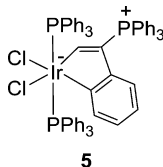
Preparation of Benzo-iridacyclopentadiene 5. Tetrabutylammonium chloride (225 mg, 0.81 mmol) and trimethylamine oxide (61 mg, 0.81 mmol) were added to a solution of **1** (200 mg, 0.16 mmol) in chloroform (10 mL). The mixture was heated to 80 °C in a Schlenk tube for 24 h. The volume of the solution was evaporated to approximately 1 mL under vacuum. Addition of ether (10 mL) to the solution gave a yellow precipitate. After filtration, the crude product was subjected to column chromatography (alumina gel, eluted with dichloromethane). Complex **5** was obtained as a light yellow solid (127 mg, 68%). ^{1}H NMR (500.2 MHz, CDCl$_3$): δ = 10.1 (d, $^3J_{PH}$ = 19.0 Hz, 1 H, IrCH), 6.8−7.8 (m, 45 H, PPh$_3$), 6.3 (d, $^3J_{HH}$ = 7.9 Hz, 1 H, IrCCH), 6.2 (dd, apparent t, $^3J_{HH}$ = 7.6 Hz, 1 H, IrCCHCH), 6.0 (d, $^3J_{HH}$ = 7.6 Hz, 1 H, IrCCHCHCHCH), 5.7 (dd, apparent t,, $^3J_{HH}$ = 7.3 Hz, 1 H, IrCCHCHCH). ^{31}P NMR (202.5 MHz, CDCl$_3$): δ = 10.2 (s, CPPh$_3$), −5.8 ppm (s, IrPPh$_3$). ^{13}C NMR plus HSQC (125.8 MHz, CD$_2$Cl$_2$): δ = 197.1 (br, IrCH), 151.6 (d, $^2J_{PC}$ = 20.7 Hz, IrCHC(PPh$_3$)C), 146.1 (br, IrC) 118.0−136.0 (m, PPh$_3$), 134.8 (s, IrCCH), 124.4 (s, IrCCHCHCH), 120.4 (s, IrCCHCHCHCH), 119.4 (s, IrCCHCH), 115.8 ppm (d, $^1J_{PC}$ = 74.2 Hz, IrCHC(PPh$_3$)). HR-MS (ESI): m/z [M − Cl]$^+$ calcd for C$_{62}$H$_{50}$ClIrP$_3$ 1115.2438, found 1115.2445. Calcd for C$_{62}$H$_{50}$Cl$_2$IrP$_3$: C, 64.69; H, 4.38. Found: C, 64.79; H, 4.27.
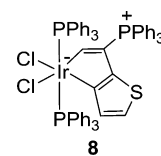

6
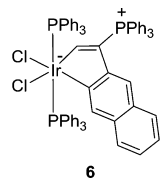
Preparation of Naphtho-iridacyclopentadiene 6. Tetrabutylammonium chloride (217 mg, 0.78 mmol) and trimethylamine oxide (59 mg, 0.79 mmol) were added to a solution of **3** (200 mg, 0.16 mmol) in chloroform (10 mL). The mixture was heated to 80 °C in a Schlenk tube for 24 h. The volume of the solution was evaporated to approximately 1 mL under vacuum. Addition of ether (10 mL) to the solution gave a yellow precipitate. After filtration, the crude product was subjected to column chromatography (alumina gel, eluted with dichloromethane). Complex **6** was obtained as a yellow solid (118 mg, 63%). ^{1}H NMR (500.2 MHz, CDCl$_3$): δ = 10.6 (d, $^3J_{PH}$ = 19.1 Hz, 1 H, IrCH), 6.3−7.8 (m, 51 H, PPh$_3$ and naphthyl). ^{31}P NMR (202.5 MHz, CDCl$_3$): δ = 10.7 (s, CPPh$_3$), −5.5 ppm (s, IrPPh$_3$). ^{13}C NMR plus HSQC (213.8 MHz, CD$_2$Cl$_2$): δ = 199.5 (s, IrCH), 152.6 (d, $^2J_{PC}$ = 19.7 Hz, IrCHC(PPh$_3$)C), 144.2 (br, IrC) 116.0−135.0 (m, PPh$_3$ and Naphthyl), 115.2 ppm (d, $^1J_{PC}$ = 75.5 Hz, IrCHC(PPh$_3$)). HR-MS (ESI): m/z [M − Cl]$^+$ calcd for C$_{66}$H$_{52}$ClIrP$_3$ 1165.2595,

found 1165.2615. Calcd for C$_{66}$H$_{52}$Cl$_2$IrP$_3$: C, 66.00; H, 4.36. Found: C, 66.07; H, 4.40.

7

Preparation of Pyreno-iridacyclopentadiene 7. Tetrabutylammonium chloride (204 mg, 0.73 mmol) and trimethylamine oxide (56 mg, 0.75 mmol) were added to a solution of **3** (200 mg, 0.15 mmol) in chloroform (10 mL). The mixture was heated to 80 °C in a Schlenk tube for 24 h. The volume of the solution was evaporated to approximately 1 mL under vacuum. Addition of ether (10 mL) to the solution gave a brown precipitate. After filtration, the crude product was subjected to column chromatography (alumina gel, eluted with dichloromethane). Complex **7** was obtained as an orange solid (77 mg, 41%). ^{1}H NMR (500.2 MHz, CDCl$_3$): δ = 11.1 (d, $^3J_{PH}$ = 21.2 Hz, 1 H, IrCH), 6.4−7.8 ppm (m, 53 H, PPh$_3$ and pyrenyl). ^{31}P NMR (202.5 MHz, CDCl$_3$): δ = 19.1 (s, CPPh$_3$), − 6.4 ppm (s, IrPPh$_3$). ^{13}C NMR was not obtained due to its poor solubility. HR-MS (ESI): m/z [M − Cl]$^+$ calcd for C$_{72}$H$_{54}$ClIrP$_3$ 1239.2751, found 1239.2766. Calcd for C$_{72}$H$_{54}$Cl$_2$IrP$_3$: C, 67.81; H, 4.27. Found: C, 67.72; H, 4.13.

8

Preparation of Thieno-iridacyclopentadiene 8. Tetrabutylammonium chloride (225 mg, 0.81 mmol) and trimethylamine oxide (61 mg, 0.81 mmol) were added to a solution of **4** (200 mg, 0.16 mmol) in chloroform (10 mL). The mixture was heated to 80 °C in a Schlenk tube for 24 h. The volume of the solution was evaporated to approximately 1 mL under vacuum. Addition of ether (10 mL) to the solution gave a yellow precipitate. After filtration, the crude product was subjected to column chromatography (alumina gel, eluted with dichloromethane). Complex **8** was obtained as a yellow solid (121 mg, 65%). ^{1}H NMR (500.2 MHz, CD$_2$Cl$_2$): δ = 10.0 (d, $^3J_{PH}$ = 18.3 Hz, 1 H, IrCH), 6.8−7.7 (m, 45 H, PPh$_3$), 6.2(d, $^3J_{HH}$ = 4.7 Hz, 1 H, SCH), 5.5 ppm (d, $^3J_{HH}$ = 4.6 Hz, 1 H, SCHCH). ^{31}P NMR (202.5 MHz, CD$_2$Cl$_2$): δ = 8.5 (s, CPPh$_3$), −7.9 ppm (s, IrPPh$_3$). ^{13}C NMR plus HSQC (125.8 MHz, CD$_2$Cl$_2$): δ = 191.3 (br, IrCH), 142.2 (br, IrC), 137.7 (d, $^2J_{PC}$ = 20.5 Hz, IrCHC(PPh$_3$)C), 119.0−135.0 (m, PPh$_3$), 131.1 (s, SCHCH), 120.0 (s, SCH), 111.4 ppm (d, $^1J_{PC}$ = 83.5 Hz, IrCHC(PPh$_3$)). HR-MS (ESI): m/z [M − Cl]$^+$ calcd for C$_{60}$H$_{48}$ClIrP$_3$ 1121.2002, found 1121.2023. C$_{60}$H$_{48}$Cl$_2$IrP$_3$S: C, 62.28; H, 4.18. Found: C, 62.03; H, 3.85.

9
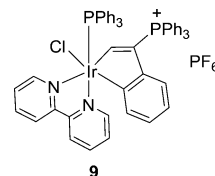
Preparation of Complex 9. 2,2′-Bipyridyl (70 mg, 0.45 mmol) and sodium hexafluorophosphate (75 mg, 0.45 mmol) were added to a solution of **5** (100 mg, 0.087 mmol) in chloroform (10 mL). The mixture was heated to 60 °C in a Schlenk tube for 2 days. The volume of the solution was evaporated to approximately 1 mL under vacuum. Addition of *n*-hexane (10 mL) to the solution gave a yellowish green precipitate. After filtration, the crude product was subjected to column chromatography (alumina gel; eluted with dichloromethane/acetone, 1:30 v/v). Complex **9** was obtained as a yellowish green solid (88 mg, 88%). ^{1}H NMR (500.2 MHz, CD$_2$Cl$_2$): δ = 9.9 (d, $^3J_{PH}$ = 19.9 Hz, 1

H, IrC*H*), 7.9–8.9 (m, 6 H, bipyridyl), 6.8–7.7 (m, 30 H, PPh$_3$; 2 H, bipyridyl), 5.3–6.4 (m, 4 H, phenyl). ^{31}P NMR (202.5 MHz, CD$_2$Cl$_2$): δ = 11.6 (s, C*P*Ph$_3$), − 10.2 ppm (s, Ir*P*Ph$_3$). ^{13}C NMR plus HSQC (125.8 MHz, CD$_2$Cl$_2$): δ = 192.7 (d, $^2J_{PC}$ = 9.98 Hz, Ir*C*H), 155.8, 155.5, 152.7, 152.3, 149.5 (s, bipyridyl), 151.8 (d, $^2J_{PC}$ = 19.3 Hz, IrCH*C*(PPh$_3$)*C*), 145.2 (dd, $^2J_{PC}$ = 18.8 Hz, $^3J_{PC}$ = 6.4 Hz, Ir*C*), 120.0–139.0 (m, PPh$_3$, phenyl, and bipyridyl), 119.3 ppm (d, $^1J_{PC}$ = 87.4 Hz, IrCH*C*(PPh$_3$)). HR-MS (ESI): m/z [M]$^+$ calcd for C$_{54}$H$_{43}$ClIrN$_2$P$_2$ 1009.2214, found 1009.2214. C$_{54}$H$_{43}$ClF$_6$IrN$_2$P$_3$: C, 56.18; H, 3.75; N, 2.43. Found: C, 56.17; H, 3.54; N, 2.50.

Crystallographic Analysis. Crystals suitable for X-ray diffraction were grown from CH$_2$Cl$_2$ or CHCl$_3$ solutions layered with *n*-hexane for **1**, **3**, **5**, **6**, **7**, **8**, and **9**. Data collections for **1**, **3**, and **8** were performed on an Oxford Gemini S Ultra CCD Area Detector using graphite-monochromated MoKα radiation (λ = 0.71073 Å) at 173 K (**1** and **3**) or at 128 K (**8**). Data collection for **5**, **6**, **7**, and **9** were collected on a Rigaku R-AXIS SPIDER IP CCD Area Detector using graphite-monochromated MoKα radiation (λ = 0.71073 Å) at 173 K. Multiscan absorption corrections (SADABS) were applied. All structures were solved by direct methods, expanded by difference Fourier syntheses, and refined by full-matrix least-squares on F^2 using the Bruker SHELXTL-97 program package. Non-H atoms were refined anisotropically unless otherwise stated. Hydrogen atoms were introduced at their geometric positions and refined as riding atoms. Further details on crystal data, data collection, and refinements are summarized in Table S1. CCDC-892086 (**1**), 892087 (**3**), 892088 (**5**), 892089 (**6**), 892090 (**7**), 892091 (**8**), and 1029774 (**9**) contain the supplementary crystallographic data for this paper. These data can be obtained free of charge from The Cambridge Crystallographic Data Centre via www.ccdc.cam.ac.uk/data_request/cif.

■ ASSOCIATED CONTENT

ⓢ Supporting Information

CIF and checkCIF files giving crystallographic data of complexes **1**, **3**, **5**, **6**, **7**, **8**, and **9**. The Supporting Information is available free of charge on the ACS Publications website at DOI: 10.1021/acs.organomet.5b00652.

> Crystallographic data of complexes **1**, **3**, **5**, **6**, **7**, **8**, and **9**, thermal stability tests of complexes **5**, **6**, **7**, and **8**, photophysical properties, GC chromatograms, TD-DFT simulations, and NMR spectra (PDF)
> Crystallographic details of complexes **1**, **3**, **5**, **6**, **7**, **8**, and **9** (CIF)

■ AUTHOR INFORMATION

Corresponding Authors
*(S.L.) E-mail: lishua@xmu.edu.cn.
*(H.X.) E-mail: hpxia@xmu.edu.cn.
Author Contributions
∥H.X. and Z.-A.H. contributed equally to this work.
Notes
The authors declare no competing financial interest.

■ ACKNOWLEDGMENTS

■ REFERENCES

(1) (a) Lamansky, S.; Djurovich, P.; Murphy, D.; Abdel-Razzaq, F.; Lee, H.-E.; Adachi, C.; Burrows, P. E.; Forrest, S. R.; Thompson, M. E. *J. Am. Chem. Soc.* **2001**, *123*, 4304−4312. (b) Lowry, M. S.; Bernhard,

S. *Chem. - Eur. J.* **2006**, *12*, 7970−7977. (c) Finkenzeller, W. J.; Hofbeck, T.; Thompson, M. E.; Yersin, H. *Inorg. Chem.* **2007**, *46*, 5076−5083. (d) You, Y.; Park, S. Y. *Dalton Trans.* **2009**, 1267−1282. (e) Ulbricht, C.; Beyer, B.; Friebe, C.; Winter, A.; Schubert, U. S. *Adv. Mater.* **2009**, *21*, 4418−4441. (f) Zhao, Q.; Huang, C.; Li, F. *Chem. Soc. Rev.* **2011**, *40*, 2508−2524. (g) You, Y.; Nam, W. *Chem. Soc. Rev.* **2012**, *41*, 7061−7084. (h) Maity, A.; Anderson, B. L.; Deligonul, N.; Gray, T. G. *Chem. Sci.* **2013**, *4*, 1175−1181.

(2) (a) Palmer, J. H.; Durrell, A. C.; Gross, Z.; Winkler, J. R.; Gray, H. B. *J. Am. Chem. Soc.* **2010**, *132*, 9230−9231. (b) Lu, K.-Y.; Chou, H.-H.; Hsieh, C.-H.; Yang, Y.-H. O.; Tsai, H.-R.; Tsai, H.-Y.; Hsu, L.-C.; Chen, C.-Y.; Chen, I. C.; Cheng, C.-H. *Adv. Mater.* **2011**, *23*, 4933−4937. (c) Palmer, J. H.; Brock-Nannestad, T.; Mahammed, A.; Durrell, A. C.; Vander Velde, D.; Virgil, S.; Gross, Z.; Gray, H. B. *Angew. Chem., Int. Ed.* **2011**, *50*, 9433−9436. (d) You, Y. *Curr. Opin. Chem. Biol.* **2013**, *17*, 699−707. (e) Zhang, G.; Zhang, H.; Gao, Y.; Tao, R.; Xin, L.; Yi, J.; Li, F.; Liu, W.; Qiao, J. *Organometallics* **2014**, *33*, 61−68.

(3) (a) Slinker, J. D.; Gorodetsky, A. A.; Lowry, M. S.; Wang, J.; Parker, S.; Rohl, R.; Bernhard, S.; Malliaras, G. G. *J. Am. Chem. Soc.* **2004**, *126*, 2763−2767. (b) Yang, C.-H.; Cheng, Y.-M.; Chi, Y.; Hsu, C.-J.; Fang, F.-C.; Wong, K.-T.; Chou, P.-T.; Chang, C.-H.; Tsai, M.-H.; Wu, C.-C. *Angew. Chem., Int. Ed.* **2007**, *46*, 2418−2421. (c) Chiu, Y.-C.; Hung, J.-Y.; Chi, Y.; Chen, C.-C.; Chang, C.-H.; Wu, C.-C.; Cheng, Y.-M.; Yu, Y.-C.; Lee, G.-H.; Chou, P.-T. *Adv. Mater.* **2009**, *21*, 2221−2225. (d) Mi, B. X.; Wang, P. F.; Gao, Z. Q.; Lee, C. S.; Lee, S. T.; Hong, H. L.; Chen, X. M.; Wong, M. S.; Xia, P. F.; Cheah, K. W.; Chen, C. H.; Huang, W. *Adv. Mater.* **2009**, *21*, 339−343. (e) Wu, C.; Chen, H.-F.; Wong, K.-T.; Thompson, M. E. *J. Am. Chem. Soc.* **2010**, *132*, 3133−3139. (f) Lee, S.; Kim, S.-O.; Shin, H.; Yun, H.-J.; Yang, K.; Kwon, S.-K.; Kim, J.-J.; Kim, Y.-H. *J. Am. Chem. Soc.* **2013**, *135*, 14321−14328.

(4) (a) Dragonetti, C.; Righetto, S.; Roberto, D.; Ugo, R.; Valore, A.; Fantacci, S.; Sgamellotti, A.; De Angelis, F. *Chem. Commun.* **2007**, 4116−4118. (b) Aubert, V.; Ordronneau, L.; Escadeillas, M.; Williams, J. A. G.; Boucekkine, A.; Coulaud, E.; Dragonetti, C.; Righetto, S.; Roberto, D.; Ugo, R.; Valore, A.; Singh, A.; Zyss, J.; Ledoux-Rak, I.; Le Bozec, H.; Guerchais, V. *Inorg. Chem.* **2011**, *50*, 5027−5038. (c) Massue, J.; Olesiak-Banska, J.; Jeanneau, E.; Aronica, C.; Matczyszyn, K.; Samoc, M.; Monnereau, C.; Andraud, C. *Inorg. Chem.* **2013**, *52*, 10705−10707. (d) Li, Y.; Dandu, N.; Liu, R.; Kilina, S.; Sun, W. *Dalton Trans.* **2014**, *43*, 1724−1735. (e) Li, Z.; Cui, P.; Wang, C.; Kilina, S.; Sun, W. *J. Phys. Chem. C* **2014**, *118*, 28764−28775.

(5) (a) Gao, R.; Ho, D. G.; Hernandez, B.; Selke, M.; Murphy, D.; Djurovich, P. I.; Thompson, M. E. *J. Am. Chem. Soc.* **2002**, *124*, 14828−14829. (b) Djurovich, P. I.; Murphy, D.; Thompson, M. E.; Hernandez, B.; Gao, R.; Hunt, P. L.; Selke, M. *Dalton Trans.* **2007**, 3763−3770. (c) Sato, S.; Morikawa, T.; Kajino, T.; Ishitani, O. *Angew. Chem., Int. Ed.* **2013**, *52*, 988−992. (d) Matt, B.; Xiang, X.; Kaledin, A. L.; Han, N.; Moussa, J.; Amouri, H.; Alves, S.; Hill, C. L.; Lian, T.; Musaev, D. G.; Izzet, G.; Proust, A. *Chem. Sci.* **2013**, *4*, 1737−1745. (e) Whang, D. R.; Sakai, K.; Park, S. Y. *Angew. Chem., Int. Ed.* **2013**, *52*, 11612−11615. (f) Jin, J.; Shin, H.-W.; Park, J. H.; Park, J. H.; Kim, E.; Ahn, T. K.; Ryu, D. H.; Son, S. U. *Organometallics* **2013**, *32*, 3954−3959.

(6) (a) Chen, H.; Zhao, Q.; Wu, Y.; Li, F.; Yang, H.; Yi, T.; Huang, C. *Inorg. Chem.* **2007**, *46*, 11075−11081. (b) You, Y.; Park, S. Y. *Adv. Mater.* **2008**, *20*, 3820−3826. (c) Zhao, Q.; Li, F.; Liu, S.; Yu, M.; Liu, Z.; Yi, T.; Huang, C. *Inorg. Chem.* **2008**, *47*, 9256−9264. (d) Liu, Y.; Li, M.; Zhao, Q.; Wu, H.; Huang, K.; Li, F. *Inorg. Chem.* **2011**, *50*, 5969−5977. (e) Chen, K.; Schmittel, M. *Chem. Commun.* **2014**, *50*, 5756−5759.

(7) (a) Yu, M.; Zhao, Q.; Shi, L.; Li, F.; Zhou, Z.; Yang, H.; Yi, T.; Huang, C. *Chem. Commun.* **2008**, 2115−2117. (b) Zhao, Q.; Yu, M.; Shi, L.; Liu, S.; Li, C.; Shi, M.; Zhou, Z.; Huang, C.; Li, F. *Organometallics* **2010**, *29*, 1085−1091. (c) You, Y.; Han, Y.; Lee, Y.-M.; Park, S. Y.; Nam, W.; Lippard, S. J. *J. Am. Chem. Soc.* **2011**, *133*, 11488−11491. (d) Maity, A.; Choi, J.-S.; Teets, T. S.; Deligonul, N.;

Berdis, A. J.; Gray, T. G. *Chem. - Eur. J.* **2013**, *19*, 15924−15932. (e) Woo, H.; Cho, S.; Han, Y.; Chae, W.-S.; Ahn, D.-R.; You, Y.; Nam, W. *J. Am. Chem. Soc.* **2013**, *135*, 4771−4787. (f) Shi, H.; Sun, H.; Yang, H.; Liu, S.; Jenkins, G.; Feng, W.; Li, F.; Zhao, Q.; Liu, B.; Huang, W. *Adv. Funct. Mater.* **2013**, *23*, 3268−3276. (g) Tang, Y.; Yang, H.-R.; Sun, H.-B.; Liu, S.-J.; Wang, J.-X.; Zhao, Q.; Liu, X.-M.; Xu, W.-J.; Li, S.-B.; Huang, W. *Chem. - Eur. J.* **2013**, *19*, 1311−1319. (h) You, Y.; Cho, S.; Nam, W. *Inorg. Chem.* **2014**, *53*, 1804−1815.

(8) (a) Bleeke, J. R.; Peng, W. J. *Organometallics* **1987**, *6*, 1576−1578. (b) Hughes, R. P.; Trujillo, H. A.; Rheingold, A. L. *J. Am. Chem. Soc.* **1993**, *115*, 1583−1585. (c) Veltheer, J. E.; Burger, P.; Bergman, R. G. *J. Am. Chem. Soc.* **1995**, *117*, 12478−12488. (d) Paneque, M.; Poveda, M. L.; Rendón, N.; Mereiter, K. *J. Am. Chem. Soc.* **2004**, *126*, 1610−1611. (e) Bleeke, J. R. *Acc. Chem. Res.* **2007**, *40*, 1035−1047. (f) Paneque, M.; Posadas, C. M.; Poveda, M. L.; Rendón, N.; Santos, L. L.; Álvarez, E.; Salazar, V.; Mereiter, K.; Oñate, E. *Organometallics* **2007**, *26*, 3403−3415. (g) Paneque, M.; Poveda, M. L.; Rendón, N.; Álvarez, E.; Carmona, E. *Eur. J. Inorg. Chem.* **2007**, *2007*, 2711−2720. (h) Álvarez, E.; Hernández, Y. A.; López-Serrano, J.; Maya, C.; Paneque, M.; Petronilho, A.; Poveda, M. L.; Salazar, V.; Vattier, F.; Carmona, E. *Angew. Chem., Int. Ed.* **2010**, *49*, 3496−3499. (i) Conejero, S.; Paneque, M.; Poveda, M. L.; Santos, L. L.; Carmona, E. *Acc. Chem. Res.* **2010**, *43*, 572−580. (j) Lin, Y.; Xu, H.; Gong, L.; Wen, T. B.; He, X.-M.; Xia, H. *Organometallics* **2010**, *29*, 2904−2910. (k) Paneque, M.; Poveda, M. L.; Rendón, N. *Eur. J. Inorg. Chem.* **2011**, *2011*, 19−33. (l) Vivancos, Á.; Paneque, M.; Poveda, M. L.; Álvarez, E. *Angew. Chem., Int. Ed.* **2013**, *52*, 10068−10071.

(9) (a) Zhang, H.; Wu, L.; Lin, R.; Zhao, Q.; He, G.; Yang, F.; Wen, T. B.; Xia, H. *Chem. - Eur. J.* **2009**, *15*, 3546−3559. (b) Zhao, Q.; Gong, L.; Xu, C.; Zhu, J.; He, X.; Xia, H. *Angew. Chem., Int. Ed.* **2011**, *50*, 1354−1358. (c) Zhu, C.; Cao, X.-Y.; Xia, H. *Youji Huaxue* **2013**, *33*, 657−662. (d) Zhu, C.; Li, S.; Luo, M.; Zhou, X.; Niu, Y.; Lin, M.; Zhu, J.; Cao, Z.; Lu, X.; Wen, T.; Xie, Z.; Schleyer, P. v. R.; Xia, H. *Nat. Chem.* **2013**, *5*, 698−703. (e) Zhu, C.; Luo, M.; Zhu, Q.; Zhu, J.; Schleyer, P. v. R.; Wu, J. I. C.; Lu, X.; Xia, H. *Nat. Commun.* **2014**, *5*, 3265. (f) Zhu, C.; Zhu, Q.; Fan, J.; Zhu, J.; He, X.; Cao, X.-Y.; Xia, H. *Angew. Chem., Int. Ed.* **2014**, *53*, 6232−6236.

(10) (a) Chi, Y.; Chou, P.-T. *Chem. Soc. Rev.* **2010**, *39*, 638−655. (b) Zhao, Q.; Liu, S.-J.; Huang, W. *Macromol. Rapid Commun.* **2010**, *31*, 794−807. (c) Guerchais, V.; Fillaut, J.-L. *Coord. Chem. Rev.* **2011**, *255*, 2448−2457. (d) Ma, D.-L.; Chan, D. S.-H.; Leung, C.-H. *Acc. Chem. Res.* **2014**, *47*, 3614−3631. (e) Chirdon, D. N.; Transue, W. J.; Kagalwala, H. N.; Kaur, A.; Maurer, A. B.; Pintauer, T.; Bernhard, S. *Inorg. Chem.* **2014**, *53*, 1487−1499. (f) Maity, A.; Stanek, R. J.; Anderson, B. L.; Zeller, M.; Hunter, A. D.; Moore, C. E.; Rheingold, A. L.; Gray, T. G. *Organometallics* **2015**, *34*, 109−120.

(11) Nonoyama, M. *Bull. Chem. Soc. Jpn.* **1974**, *47*, 767−768.

(12) On the basis of a search of the Cambridge Structural Database, CSD version 5.36 (Feb 2015).

(13) (a) Wolowiec, S.; Kochi, J. K. *Inorg. Chem.* **1991**, *30*, 1215−1221. (b) Berkessel, A.; Reichau, S.; von der Höh, A.; Leconte, N.; Neudörfl, J.-M. *Organometallics* **2011**, *30*, 3880−3887.

(14) (a) Liu, B.; Xie, H.; Wang, H.; Wu, L.; Zhao, Q.; Chen, J.; Wen, T. B.; Cao, Z.; Xia, H. *Angew. Chem., Int. Ed.* **2009**, *48*, 5461−5464. (b) Musa, S.; Shaposhnikov, I.; Cohen, S.; Gelman, D. *Angew. Chem., Int. Ed.* **2011**, *50*, 3533−3537.

(15) Werner, H.; Hohn, A. *J. Organomet. Chem.* **1984**, *272*, 105−113.

(16) Bierstedt, A.; Clark, G. R.; Roper, W. R.; Wright, L. J. *J. Organomet. Chem.* **2006**, *691*, 3846−3852.

(17) Choudhury, J.; Pratihar, S.; Maity, A. K.; Roy, S. *Can. J. Chem.* **2009**, *87*, 183−187.

(18) Vivancos, Á.; Hernández, Y. A.; Paneque, M.; Poveda, M. L.; Salazar, V.; Álvarez, E. *Organometallics* **2015**, *34*, 177−188.

(19) (a) Chirdon, D. N.; McCusker, C. E.; Castellano, F. N.; Bernhard, S. *Inorg. Chem.* **2013**, *52*, 8795−8804. (b) Deligonul, N.; Browne, A. R.; Golen, J. A.; Rheingold, A. L.; Gray, T. G. *Organometallics* **2014**, *33*, 637−643. (c) Zhou, Y.; Gao, H.; Wang, X.; Qi, H. *Inorg. Chem.* **2015**, *54*, 1446−1453. (d) Li, T.-Y.; Liang, X.; Zhou, L.; Wu, C.; Zhang, S.; Liu, X.; Lu, G.-Z.; Xue, L.-S.; Zheng, Y.-X.; Zuo, J.-L. *Inorg. Chem.* **2015**, *54*, 161−173. (e) Nguyen, V. H.; Khoo, R. S. H.; Yip, J. H. K. *Inorg. Chem.* **2015**, *54*, 2264−2277.

(20) (a) Olgemöller, B.; Bauer, H.; Beck, W. *J. Organomet. Chem.* **1981**, *213*, C57−C59. (b) Neenan, T. X.; Whitesides, G. M. *J. Org. Chem.* **1988**, *53*, 2489−2496.

(21) (a) Lee, C.; Yang, W.; Parr, R. G. *Phys. Rev. B: Condens. Matter Mater. Phys.* **1988**, *37*, 785−789. (b) Becke, A. D. *J. Chem. Phys.* **1993**, *98*, 5648−5652.

(22) Frisch, M. J.; Trucks, G. W.; Schlegel, H. B.; Scuseria, G. E.; Robb, M. A.; Cheeseman, J. R.; Scalmani, G.; Barone, V.; Mennucci, B.; Petersson, G. A.; Nakatsuji, H.; Caricato, M.; Li, X.; Hratchian, H. P.; Izmaylov, A. F.; Bloino, J.; Zheng, G.; Sonnenberg, J. L.; Hada, M.; Ehara, M.; Toyota, K.; Fukuda, R.; Hasegawa, J.; Ishida, M.; Nakajima, T.; Honda, Y.; Kitao, O.; Nakai, H.; Vreven, T.; Montgomery, J. A., Jr.; Peralta, J. E.; Ogliaro, F.; Bearpark, M.; Heyd, J. J.; Brothers, E.; Kudin, K. N.; Staroverov, V. N.; Keith, T.; Kobayashi, R.; Normand, J.; Raghavachari, K.; Rendell, A.; Burant, J. C.; Iyengar, S. S.; Tomasi, J.; Cossi, M.; Rega, N.; Millam, J. M.; Klene, M.; Knox, J. E.; Cross, J. B.; Bakken, V.; Adamo, C.; Jaramillo, J.; Gomperts, R.; Stratmann, R. E.; Yazyev, O.; Austin, A. J.; Cammi, R.; Pomelli, C.; Ochterski, J. W.; Martin, R. L.; Morokuma, K.; Zakrzewski, V. G.; Voth, G. A.; Salvador, P.; Dannenberg, J. J.; Dapprich, S.; Daniels, A. D.; Farkas, Ö., Foresman, J. B.; Ortiz, J. V.; Cioslowski, J.; Fox, D. J. *Gaussian 09*, revision B.01, Gaussian, Inc.: Wallingford, CT, 2010.

(23) Huzinaga, S.; Anzelm, J.; Klobukowski, M.; Radzio-Andzelm, E.; Sakai, Y.; Tatewaki, H. *Gaussian Basis Sets for Molecular Calculations*; Elsevier: Amsterdam, 1984.